

Aeroelastic response analysis of turboprop aircraft including effects of powerplant rotating mass

J. Čečrdle^a

^a Czech Aerospace Research Centre (VZLU), Beranových 130, 199 05 Praha Letňany, Czech Republic

Aeroelastic certification analyses of turboprop aircraft are required to take in account the dynamic and aerodynamic effects of rotating masses, such as a propeller or a gas turbine engine rotor. These effects are usually considered with respect to the aeroelastic stability (whirl flutter). Nevertheless, the mentioned effects also influence the dynamic behaviour of the structure with respect to the dynamic (aeroelastic) response, especially the response of engines. Contrary to flutter, the key issue is not a structural integrity, but the issues related to static strength or fatigue life of specific structural parts (e.g. engine suspension) as dynamic responses generate dynamic loads.

Physical principle is outlined on a simple mechanical system with two degrees of freedom. A flexible engine mounting is represented by two rotational springs of stiffnesses K_ψ and K_θ , as illustrated in Fig. 1.

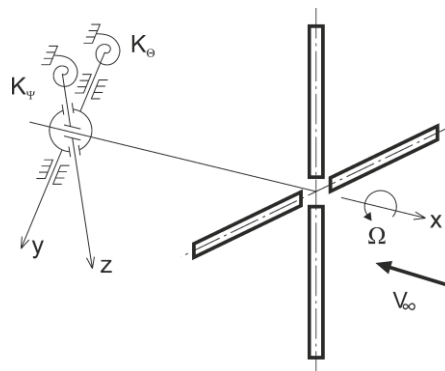


Fig. 1. Gyroscopic system with propeller

Such a system has two independent mode shapes (yaw and pitch) with angular frequencies ω_ψ and ω_θ . For a propeller rotation with angular velocity Ω , the gyroscopic effect causes both independent mode shapes to merge into a whirl motion. The axis of rotation of the propeller exhibits an elliptical movement. The orientation is backward relative to the propeller rotation for the mode with the lower frequency (backward whirl mode) and forward relative to the propeller rotation for the mode with the higher frequency (forward whirl mode). The gyroscopic motion results in changes in the propeller blades' angles of attack, consequently leading to unsteady aerodynamic forces. These forces may induce the instability. If the air velocity is lower than the critical speed, the system is stable, and the gyroscopic motion is damped (Fig. 2a). If the airspeed exceeds the critical speed, the system becomes unstable, and the gyroscopic motion is divergent (Fig. 2b).

Contrary to flutter, the right-hand side of aeroelastic response equations of motion is non-zero. Instead, frequency dependent loading is applied. Loading origin may be aerodynamic (gust, turbulence), dynamic (landing impact, store ejection, gun firing) or

combined (control surface deflection). Loading may be either in frequency domain (frequency response) or in the time domain (transient response). In both cases, the primary analysis is performed in the frequency domain. In the case of transient analysis, Fourier Transform Technique is employed to convert loads into the frequency domain and computed quantities are then converted back using Inverse Fourier Transform Technique. For both types of analysis, modal solution is employed.

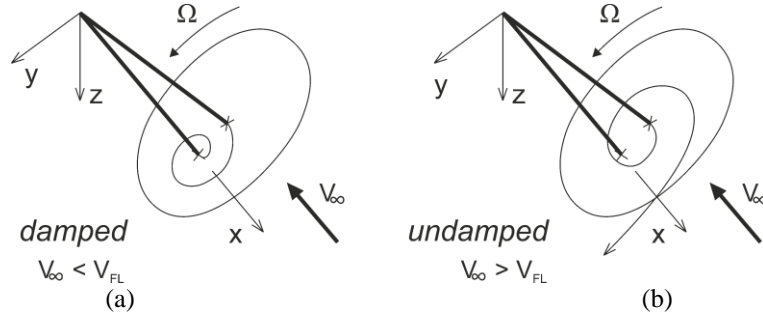


Fig. 2. Stable (a) and unstable (b) states of gyroscopic vibrations for the backward whirl mode

Matrix equation for the above-mentioned case with engine pitch and yaw modes become

$$\left[-\omega^2 [\mathbf{M}] + j\omega \left([\mathbf{D}] + [\mathbf{G}] + qF_p \frac{D_p}{V} [\mathbf{D}^A] \right) + ([\mathbf{K}] + qF_p D_p [\mathbf{K}^A]) \right] \begin{Bmatrix} \bar{\Theta} \\ \bar{\Psi} \end{Bmatrix} = \{P(\omega)\}, \quad (1)$$

where left-hand side include mass matrix, structural damping matrix, structural stiffness matrix, gyroscopic matrix representing the dynamic effect of rotating mass, and finally aerodynamic damping and stiffness matrices representing the aerodynamic effect of rotating mass. Vector of modal deformation include generalised pitch and yaw angles. Right-hand side include frequency dependent load vector.

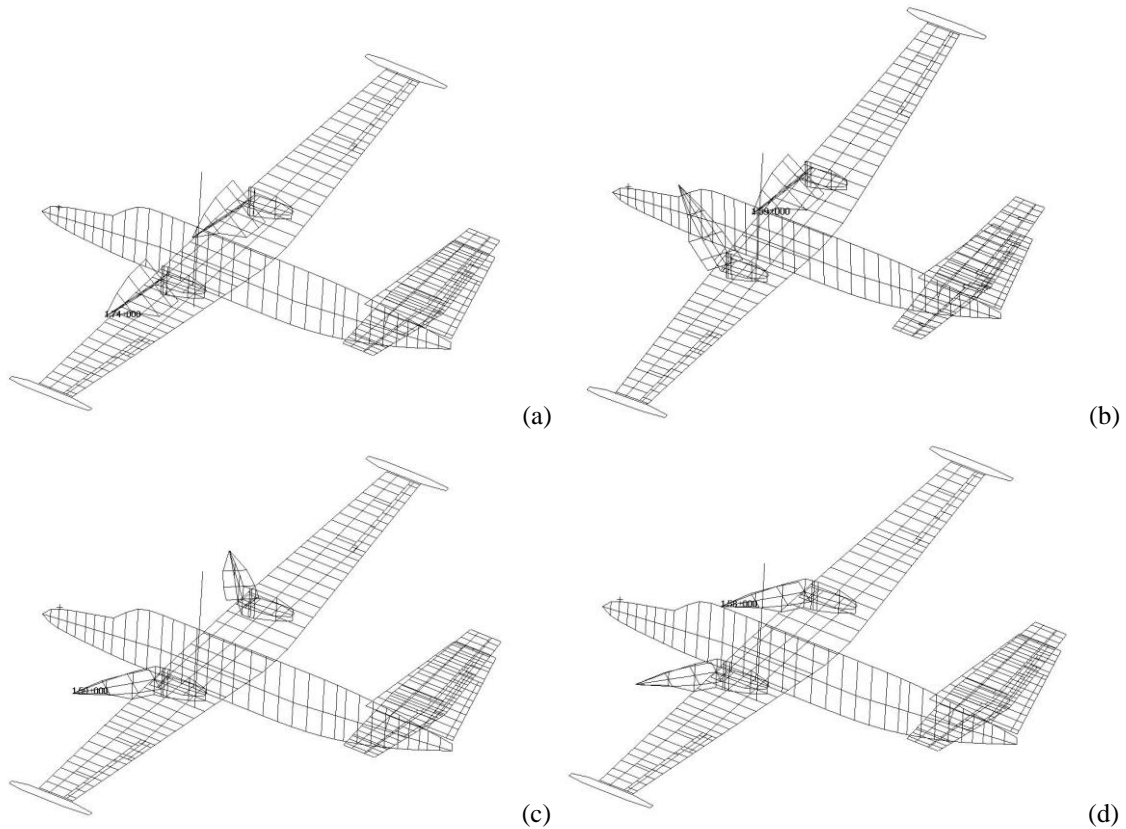


Fig. 3. Engines vibration mode shapes: (a) $S\Theta$, (b) $A\Theta$, (c) $SPsi$ and (d) $APsi$

Solution is based on a rigid propeller in a windmilling mode. Unsteady aerodynamic forces on a propeller are calculated by Strip Theory. Unsteady aerodynamic forces on a residual structure (wing and nacelles) are calculated by Wing Body Interference Theory.

Presented calculations represent analyses of a twin-engine turboprop aircraft for 19 passengers. Parameters of analyses were following: Flight altitude 4267 m, Mach number 0.493, damping ratio 0.02, flight velocities 100, 200 and 300 m/s, propellers rpm 2080. Both identical and inverse rotations of both propellers were considered. For the nominal stiffness of engines suspension, the engines show the following vibration modes: Symmetric pitch ($S\Theta$) 8.14 Hz, antisymmetric pitch ($A\Theta$) 9.89 Hz, symmetric yaw ($S\Psi$) 10.43 Hz and antisymmetric yaw ($A\Psi$) 12.21 Hz. These modes are shown in Fig. 3.

In the following examples, the displacement of the starboard engine front point is presented. First example demonstrates the frequency response to the harmonic force excitation applied to both engines. The airflow velocity was 100 m/s. Specific relations of forces were used to excite appropriate gyroscopic movement. Fig. 4 demonstrates the coupling of $S\Theta$ and $A\Psi$ modes. Fig. 4a shows the case with no propeller rotation in which two independent modes are present while Fig. 4a shows the case with CW-CW rotations of both propellers, in which both modes merge to the gyroscopic motion. Backward whirl mode has elliptical trajectory with dominating pitch deformation (T2) and the frequency is lower compare to the frequency of the uncoupled $S\Theta$ mode. Forward whirl mode has elliptical trajectory with dominating yaw deformation (T3) and the frequency is higher compare to the uncoupled $A\Psi$ mode. Similarly, Fig. 5 demonstrates the coupling of $A\Theta$ and $A\Psi$ modes. Fig. 5a shows the case with no propeller rotation in which two independent modes are present while Fig. 5a shows the case with CW-CCW rotations of both propellers, in which both modes merge to the gyroscopic motion. Backward whirl mode has elliptical trajectory with dominating pitch deformation and the frequency is lower compare to the frequency of the uncoupled $A\Theta$ mode. Forward whirl mode has elliptical trajectory with dominating yaw deformation and the frequency is higher compare to the uncoupled $A\Psi$ mode.

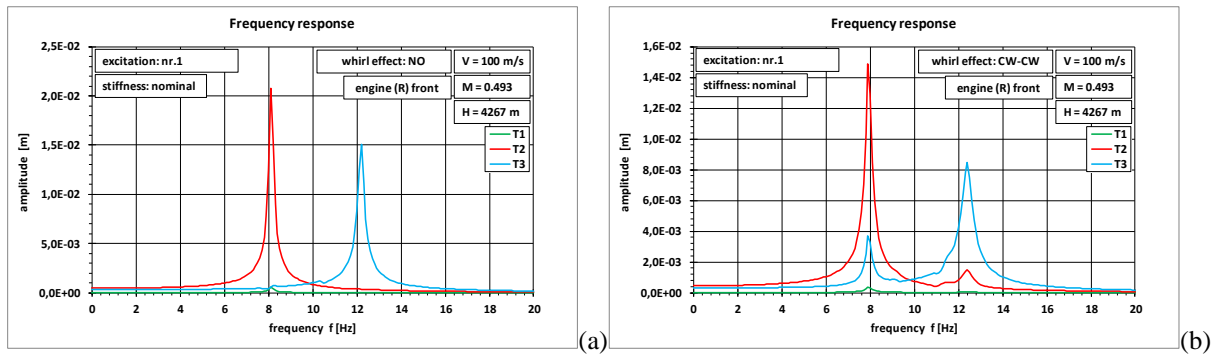


Fig. 4. Frequency response, $V = 100$ m/s, starboard engine front point, excited modes: $S\Theta$, $A\Psi$. Propellers rotation (a) no, (b) CW-CW

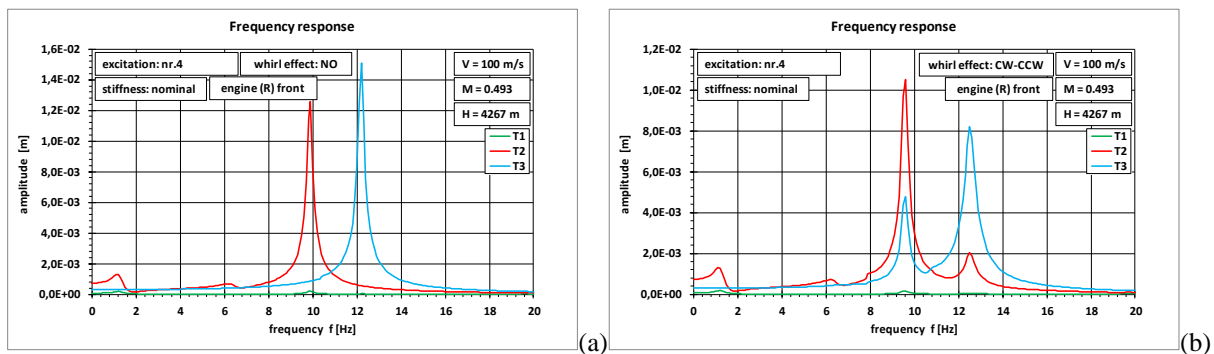


Fig. 5. Frequency response, $V = 100$ m/s, starboard engine front point, excited modes: $A\Theta$, $A\Psi$. Propellers rotation (a) no, (b) CW-CCW

The second example demonstrates the transient response to the landing impact at the velocity of 50 m/s. The excitation is realised as enforced displacement obtained from the main landing gear drop test. Fig. 6a shows the case with no propeller rotation. Fig. 6b then demonstrates the comparison of pitch displacement (T2) of the cases with no rotation, CW-CW rotation and CW-CCW rotation. Increase in damping as well as decrease in frequency can be found for both cases including rotation compare to the no rotation case.

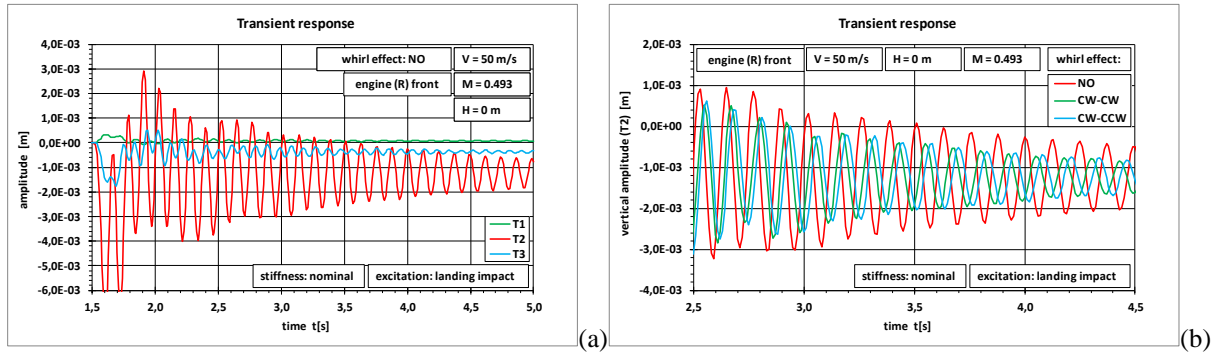


Fig. 6. Transient response, $V = 50$ m/s, starboard engine front point, landing impact excitation. (a) no propellers rotation, (b) pitch displacement (T2), comparison

The last example demonstrates the transient response to the delta impulse applied at the centre of gravity. The airflow velocity was 200 m/s. Reduced stiffness was applied to demonstrate the state of neutral stability in this example. Fig. 7a shows the response for the case with no propeller rotation in which the response is damped and both pitch (T2) and yaw (T3) deformations are independent and frequencies of pitch and yaw vibrations are diverse. Fig. 7b shows the case with CW-CW rotation in which the response is (almost) harmonic and the damping of the system is (almost) zero showing the state of the neutral stability. Also, the change in the frequency and coupling of both pitch and yaw deformations (phase shift) can be found compare to the no rotation case.

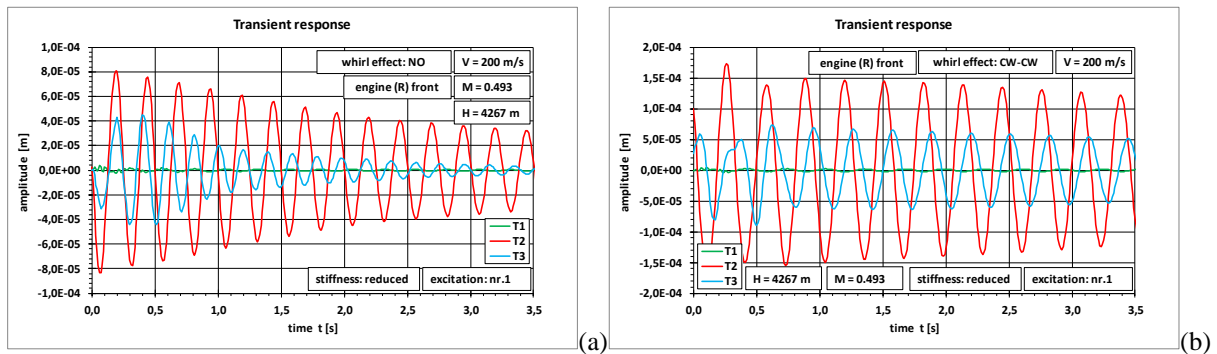


Fig. 7. Transient response, $V = 200$ m/s, starboard engine front point, delta impulse excitation. Propellers rotation (a) no, (b) CW-CW

References

- [1] Čečrdle, J., Whirl flutter of turboprop aircraft structures, Elsevier Science, Oxford, 2015.
- [2] Giessing, J.P., Kalman, T.P., Rodden, W.P., Subsonic steady and oscillatory aerodynamics for multiple interfering wings and bodies, *Journal of Aircraft* 9 (1972) 693-702.
- [3] Rodden, W.P., Bellinger, E.D., Aerodynamic lag functions, divergence, and the British flutter method, *Journal of Aircraft* 19 (1982) 596-598.
- [4] Theodorsen, T., General theory of aerodynamic instability and the mechanism of flutter, NACA Report 496, 1935.